

A Magnetic Resonance Imaging–Compatible, Large-Scale Array for Trans-Skull Ultrasound Surgery and Therapy

Gregory T. Clement, PhD, FInstP, P. Jason White, MS,
Randy L. King, MS, Nathan McDannold, PhD,
Kullervo Hynynen, PhD

Objective. Advances in ultrasound transducer array and amplifier technologies have prompted many intriguing scientific proposals for ultrasound therapy. These include both mildly invasive and noninvasive techniques to be used in ultrasound brain surgery through the skull. In previous work, it was shown how a 500-element hemisphere-shaped transducer could correct the wave distortion caused by the skull with a transducer that operates at a frequency near 0.8 MHz. Because the objective for trans-skull focusing is its ultimate use in a clinical context, a new hemispheric phased-array system has now been developed with acoustic parameters that are optimized to match the values determined in preliminary studies. **Methods.** The transducer was tested by focusing ultrasound through ex vivo human skulls and into a brain phantom by means of a phase-adaptive focusing technique. Simultaneously, the procedure was monitored by the use of magnetic resonance guidance and thermometry. **Results.** The ultrasound focus of a 500-element 30-cm-diameter, 0.81-MHz array could be steered electronically through the skull over a volume of approximately $30 \times 30 \times 26$ mm. Furthermore, temperature monitoring of the inner and outer surfaces of the skull showed that the array could coagulate targeted brain tissue without causing excessive skull heating. **Conclusions.** The successful outcome of these experiments indicates that intensities high enough to destroy brain tissue can be produced without excessive heating of the surrounding areas and without producing large magnetic resonance noise and artifacts. **Key words:** phase aberration correction; thermal imaging; trans-skull therapy; ultrasound therapy.

Abbreviations

CT, computed tomography; CW, continuous wave; MR, magnetic resonance; PZT, lead zirconate titanate

Received November 12, 2004, from the Department of Radiology, Harvard Medical School, Brigham and Women's Hospital, Boston, Massachusetts 02115. Revision requested December 15, 2004. Revised manuscript accepted for publication March 17, 2005.

This work was supported by InSightec Ltd and grant R01EB003268 from the National Institutes of Health.

Address correspondence to Gregory T. Clement, PhD, FInstP, Department of Radiology, Harvard Medical School, Brigham and Women's Hospital, 221 Longwood Ave, Room 521, Boston, MA 02115 USA.

E-mail: gclement@hms.harvard.edu

A number of studies have proposed the use of large-area ultrasound arrays as a strategy in trans-skull ultrasound brain therapies.¹⁻⁵ In this still investigational procedure, an array is created that can focus ultrasound into a precise location in the brain and destroy the tissue at the focus but still preserve the areas around it. Furthermore, it is essential that the array operate successfully in the presence of a magnetic resonance (MR) device that will be used to visualize the brain and aim the focus of the large-scale ultrasound array.²

The goal of this study was to produce a transducer that is MR compatible and able to correct for the distortion caused by the skull bone⁶ and avoid substantial skull heating during high-power sonications. To develop such an array, however, several issues of design and measurement had to be considered.

First, the number of transducer elements had to be sufficiently large to allow beam steering, to correct for ultrasound diffraction and scattering, and to deliver therapeutic power levels.⁷ Second, the surface area of the transducer had to be large enough to minimize the risk of skull heating and prevent thermally induced changes of the speed of sound in the bone.⁷ Furthermore, the frequency had to be optimized to allow maximum thermal gain between the ultrasound focus and the skull surface. It was essential that this transducer be built with minimal cross-element coupling; in addition, the materials in it could not be ferromagnetic or otherwise interfere with the MR imaging process. By addressing these problems here and in previous studies,⁷⁻¹⁰ a hemisphere-shaped transducer array design¹⁰ was chosen.

Materials and Methods

Design and Construction

Maximum distribution of energy over the skull surface was achieved by constructing the transducer in the shape of a hemisphere. The transducer diameter was 30 cm to facilitate motion of the head within the array to easily position the tumor at the geometric center of the transducer. This design also allows a relatively simple registration of the element locations. The entire transducer was segmented into 500 equally spaced elements. This use of equal-area elements simplified the power considerations for operating the array. During a simulation study,⁷ it was discovered that a phase-corrected array on the order of 500 elements would produce a focus on the order of 1 mm in diameter through a human skull at the geometric center of the transducer. Although this number of elements allows for limited electronic beam steering, the transducer design was intended primarily to provide adequate aberration correction at the geometric focus rather than electronic steering.⁸

In the clinic, a patient would be coupled to the transducer via a water interface, and the top of the patient's head would be shaved before insertion into a watertight flexible membrane. The outer part of the membrane would be attached to the perimeter of the transducer via a watertight O-ring seal. The area between the membrane and the transducer would be completely filled with degassed water to ensure good coupling and minimize the possibility of cavitation in the acoustic near field.

Previous studies have shown that the optimal thermal gain between the focus in the brain and the skull surface is reached, on average, at frequencies near 0.7 MHz.¹¹ This result was found by comparing the temperature rise at the focus with that on the skull surface; however, a considerable variation of the optimal frequency among the different skull samples in the study (0.5–0.8 MHz) was found, as well as variations up to 100 kHz on different sections of the same skull. The choice of a 1-3 piezocomposite material allows for flexibility in the transducer bandwidth without impeding the high-power continuous wave (CW) operation of the array. As an improvement on a previous hemisphere array made of lead zirconate titanate (PZT) elements,¹¹ the use of the composite material also is expected to simplify transducer construction. Because the 1-3 material consists of equally spaced thin “1-dimensional” PZT rods embedded in a 3-dimensional polymer matrix, individual elements can be defined simply by an electrode pattern and do not require physical separation of the elements.

This transducer was constructed from a custom-made 500-element, 30-cm-diameter 1-3 composite hemispheric shell (Imasonic, Besançon, France). The electrode surface was divided into 500 elements of equal area. Specifically, the array pattern consisted of a center element and 13 rings of elements, and each element was wired with 1 m of coaxial cable (8700; Belden CDT Electronics Division, Richmond, IN). A picture of the finished transducer is shown in Figure 1. The elements were initially matched individually to an electrical resonance of 0.81 MHz at 50 Ω to ensure maximum power output from the amplifier system to the transducer. A smaller, 9-element test array (Imasonic) was also constructed to facilitate acoustic laboratory tests. The elements of this 6.4-cm-diameter array were identical in area and composition to those in the 500-element array.

A previous study examined a hemisphere radiator, which was composed of 64 isolated PZT elements.¹⁰ Those experiments showed that acoustic powers exceeding 1000 W are often necessary for tissue coagulation through thicker skulls. It was expected that the thermal focal gain would be increased by extending the number of elements to 500, thereby reducing the power requirements for the new array. Thus, a conservative power rating of 1500 W of total acoustic output was chosen to ensure adequate

power. The composite material used in the array was rated at a maximum acoustic output intensity of 5 W/cm^2 .

Two separate driving systems were used to supply signals to the transducer during the array tests. The first system, manufactured in-house, was used in the laboratory to acquire ultrasound field measurements in a water tank. That amplifier allowed a maximum of 120 channels to be driven simultaneously. To measure the field from the array, acoustic pressure measurements were taken in sections and later combined numerically. This method was similar to that reported by Clement et al.⁹ In those laboratory tests, planar scans were performed with a 0.075-mm-diameter needle hydrophone (Precision Acoustics Ltd, Dorchester, Dorset, England) by means of a positioning system (VP9000; Velmex, Bloomfield, NY) accurate to $10 \mu\text{m}$. Measurements were taken over areas normal to the axis of symmetry of the transducer. Each measurement covered a 12×12 -mm area, with a sampling resolution of 0.3 mm. During experimental measurements, an electrical power of 0.05 W was supplied to each element. These measurements were compared with numeric field simulations by a discrete approximation to the Rayleigh surface integral as described previously in detail¹⁰ for the case of a 64-element hemisphere.

The second amplifier system was a subsystem of an integrated MR imaging-guided focused ultrasound surgery system (InSightec Ltd, Haifa, Israel) that was specifically designed to operate the trans-skull array within a clinical MR imaging system. This high-power MR imaging-compatible system was capable of driving all 500 channels. The system was first used to measure skull heating with thermocouples and later in a clinical MR imaging unit (LX; GE Healthcare, Waukesha, WI).

Characterization

The 9-element prototype transducer was used to measure the electrical-to-acoustic power conversion efficiency of the trans-skull transducer. The smaller size of the prototype allowed it to be affixed in a radiation force measurement tank. The electrical driving signals were generated by a synthesized function generator (DS345; Stanford Research Systems, Sunnyvale, CA), amplified by a 55-dB power amplifier (2100L; ENI Products, Rochester, NY), and then evenly distributed to

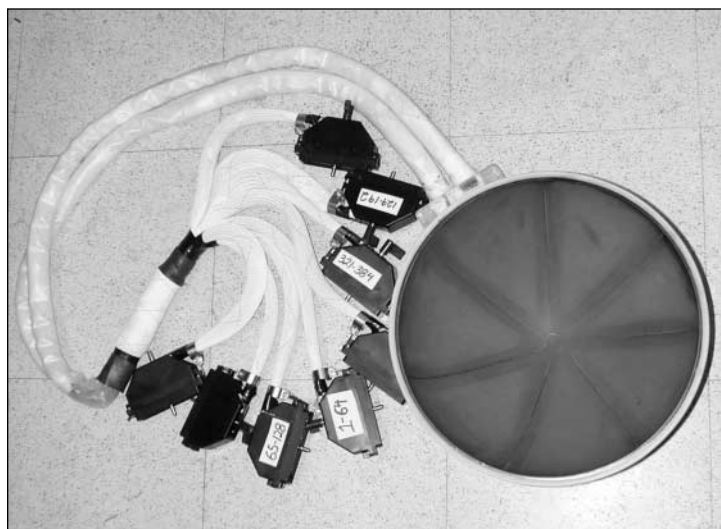


Figure 1. Picture of the 500-element hemispheric array.

each element of the transducer. During a 10-second sonication, the electrical power was measured with a power meter (438A; Hewlett-Packard Company, Palo Alto, CA), and the output acoustic power was calculated by a radiation force technique, with an absorbing target attached to a laboratory scale (AE 200; Mettler Toledo, Columbus, OH). The efficiency was calculated by dividing the acoustic power output by the input electrical power. Efficiency measurements were performed at frequencies between 0.5 and 1.1 MHz at steps of 0.1 MHz.

The steering range of the 500-element transducer was tested by a standard technique, during which the signal from each element is set in phase at the desired focal point. To perform the measurements, the 500-element transducer was fully submerged in water with its axis of symmetry parallel to the water surface. To prevent standing wave interference, the holding tank interior was covered with anechoic rubber. The 0.075-mm hydrophone was affixed to the stepping motor-controlled positioning system and placed at the location where the ultrasound was to be focused. A CW signal was then delivered to each transducer element to record the waveforms at the hydrophone. The driving phase of each signal was evaluated and automatically adjusted so that the signal of every element arrived at the hydrophone in phase. The entire phasing process was controlled with a personal computer with a general purpose interface board and took approximately 5 minutes to perform.

Focusing Through Ex Vivo Human Skulls

To test aberration correction through the skull, a human calvarium sample was inserted between the hydrophone and the transducer, with the hydrophone positioned at the 500-element geometric center of the transducer. Once a focus was obtained via the phasing method described above, it was hypothesized that a further implementation of the focusing algorithm to move the focus was not necessary. Instead, the focus was moved away from the initial focal point by a previously described approach,¹² shifting the focus from an initial point r_a to a new position at point r_b , adjusting the phase of each element by an amount as follows:

$$(1) \quad \Delta\phi(r_b) = \arg\left(\frac{P(r_a)}{P_0(r_a)} P_0(r_b)\right).$$

Here, the measurement of the field in water is given by P_0 , and the field through the skull by P . Measurements were performed in 17 successive locations perpendicular to the axis of symmetry of the transducer and then in 17 more locations along the axis. In both cases, the measurements were taken at 2-mm intervals.

The focus was also mechanically moved to new locations by repositioning the skull inside the transducer. Unlike electrical steering, the mechanical case required refocusing with the phasing algorithm at each measurement location. Initially, the shifting was performed in 8 locations placed 6.3 mm apart along the transducer axis and then in 5 locations placed 12.5 mm apart along the radial direction normal to this axis.

Thermocouple Measurements of Skull Heating

Before thermal imaging tests with MR thermometry were performed, temperature measurements were taken with thermocouples of the ultrasound focus and the inner and outer surfaces of 2 skull specimens. These experiments were performed to measure the temperature inside the bone because MR thermometry can accurately measure temperature changes in water-based materials but cannot detect heating in bone. The thermocouple measurements provided an accurate measurement of potentially dangerous skull heating relative to the desired heating at the ultrasound focus within the brain.

The outer surface of the skull was encased by a skin-mimicking phantom of approximately 0.5-mm thickness. The main composition of this phantom was based on a variant of materials described by Madesen et al¹³ and consisted primarily of condensed milk and gelatin. Trace amounts of *n*-propanol alcohol were added for sound speed adjustment, and thimerosal was added as a preservative. The skin-mimicking phantom was contained in a thin latex (wall thickness, <0.1 mm) envelope. The edges of the latex envelope were attached to the skull underwater so that air was not trapped between the phantom and the outer surface of the specimen. The inner cavity of the specimen was filled with a brain-mimicking phantom.¹³ The phantom material was heated and poured directly into the calvarium and allowed to harden to a gel at room temperature.

One constantan-copper thermocouple was embedded in the brain phantom at the focus of the transducer array; a second was embedded at the interface between the brain phantom and the inner surface of the skull; and a third was embedded at the interface between the outer surface of the skull and the skin phantom. The output of the 3 thermocouples was logged by a computer via a multimeter (2700; Keithley Instruments, Cleveland, OH).

For each skull, the transducer elements were uniquely phased according to a computed tomography (CT)-derived noninvasive focusing model.³ Temperature rise was then studied as a function of sonication time, power level, and duty cycle. For the 2 skull specimens, sonication times of 5, 10, 20, 30, and 40 seconds were performed at 1800 W and 100% duty cycle. The time between sonications (\approx 15 minutes) was sufficient for the phantom and skull to return to ambient temperature. For the same 2 specimens, 5-second sonications of 20, 40, 60, and 80 seconds (duty cycle frequency, 200 Hz) were performed at 1800 W and 100% duty cycle. For 1 specimen, 20-second sonications were performed at 100, 200, 400, 600, and 1800 W and 100% duty cycle.

Tests in a Clinical MR Imaging Scanner

Experiments next proceeded in a water-filled tank, situated within the bore of a 1.5-T clinical MR imaging unit (GE Healthcare). A stereotaxic reference frame was used to affix an ex vivo human skull to the 500-element hemispheric

transducer. The interior of the skull was filled with the brain tissue-mimicking phantom described above, and its surface was covered with the skin-mimicking phantom. To focus ultrasound through the skull and into the phantom, a previously developed phase aberration correction algorithm³ was used. The data for this algorithm were obtained from a digitized 3-dimensional rendering of the skull, achieved by the use of CT images (Somatom CT scanner; Siemens Medical Solutions, Malvern, PA) (field of view, 20 cm; slice thickness, 1 mm). Using a bone reconstruction kernel (AH82; Siemens Medical Solutions), image intensities proportional to the bone density were acquired. A description of the registration between the CT images and the transducer has been described previously.³

Next, CW sonications into the brain phantom were performed for 20 to 30 seconds at electrical powers ranging from 300 to 1200 W with the MR imaging-guided focused ultrasound system (InSightec Ltd). The sonications for the first study were performed for 20 seconds at a total electrical input power of 320 W. This procedure was repeated with 5 different skulls. Temperature images were constructed in 1 plane from phase difference images of a fast spoiled gradient echo sequence (repetition time/echo time, 51.7/25.6 milliseconds; flip angle, 30°; bandwidth, 3.1 kHz; field of view, 12 cm; slice thickness, 3 mm; matrix size, 256 × 128; scan time, 6.8 seconds). The temperature sensitivity was -0.011 ppm/°C, and a time series of temperature maps was developed.

Table 1. Efficiency of the 9-Element Composite Array

Frequency, MHz	Electric Power, W	Acoustic Power, W	Efficiency, %
0.5	6.97	0.959	13.8
0.6	7.56	2.19	29.0
0.7	7.67	4.23	55.2
0.8	7.57	4.66	61.6
0.9	7.88	3.48	44.2
1.0	7.28	2.65	36.4
1.1	7.20	2.33	32.4

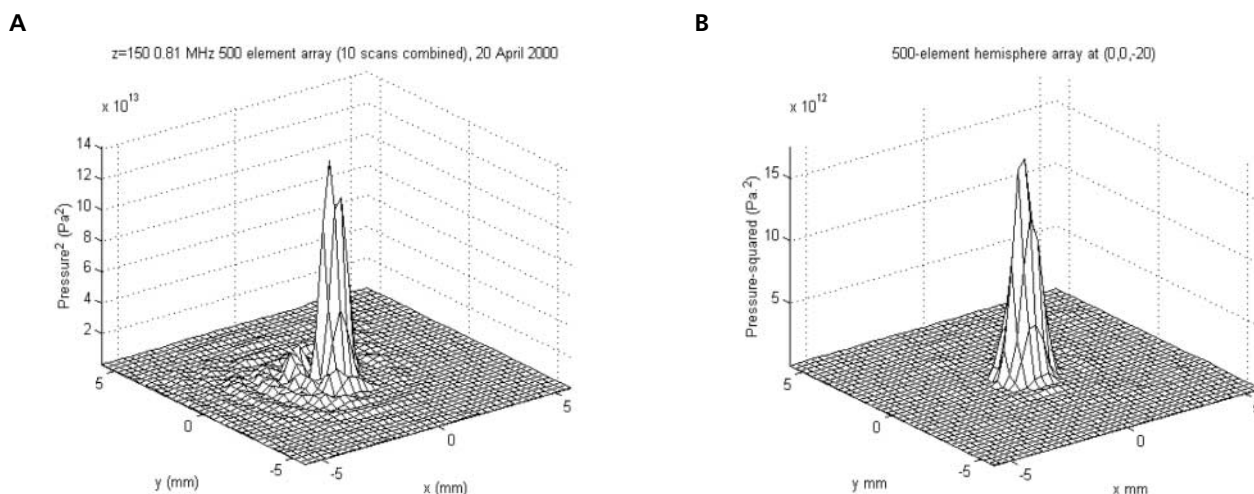
Results

Electroacoustic measurements, done with a nominal length of cable, are summarized in Table 1 and show a peak efficiency of 62% at 0.8 MHz for the 9-element prototype transducer. Because of similarities in the array construction, similar efficiencies were inferred for the 500-element transducer.

The steering range of the 500-element array, operated at 0.81 MHz, was determined from the combined hydrophone measurements. An effective range of approximately 30 × 30 × 26 mm was observed, with volume boundaries defined by a 50% drop-off of its peak acoustic intensity. Figure 2A shows the pressure-squared beam plot, with the focus at the geometric center of the transducer. The field, steered 20 mm, is shown in Figure 2B.

Next, a skull was inserted between the hydrophone and the 500-element transducer. The phasing process was repeated with the

Figure 2. Pressure-squared beam plots at the transducer's geometric center (A) and at 20 mm (B).



hydrophone located at the geometric center of the transducer. The field measured at the geometric center of the array had a focal shape almost identical to its counterpart in water without a skull; however, the peak had dropped approximately 1 order of magnitude in acoustic intensity. Next, electronic shifting was applied to this algorithm-phased field with the use of Equation 1. A shift to the intended location was observed, but it was generally accompanied by a reduction in the focal amplitude. In this steering scenario, the array served the dual role of both aberration correction and beam steering. Figure 3 shows a composite intensity plot of the central focus as well as 4 foci shifted 25 mm from the center. Circles on the plot indicate the intended focal locations. The shifted beams appear to be similar in size and shape to the on-axis focus.

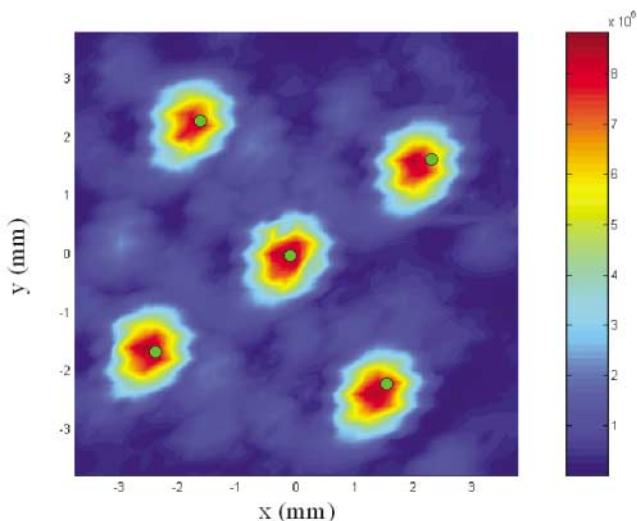
Along the axis of symmetry of the transducer, shown in Figure 4A, steering of the beam inward toward the skull surface actually resulted in a higher response for a range of approximately 10 mm before declining rapidly. In fact, an increase in signal was expected because the curvature of the skull tends to refract the focus inward. Based on a 50 % drop-off, an electronic steering range of 24 mm was recorded, which is a distance comparable with the on-axis steering range of the transducer in water. A smaller range in the radial direction was observed, as shown in Figure 4B. In this case, the 50% drop-off indicat-

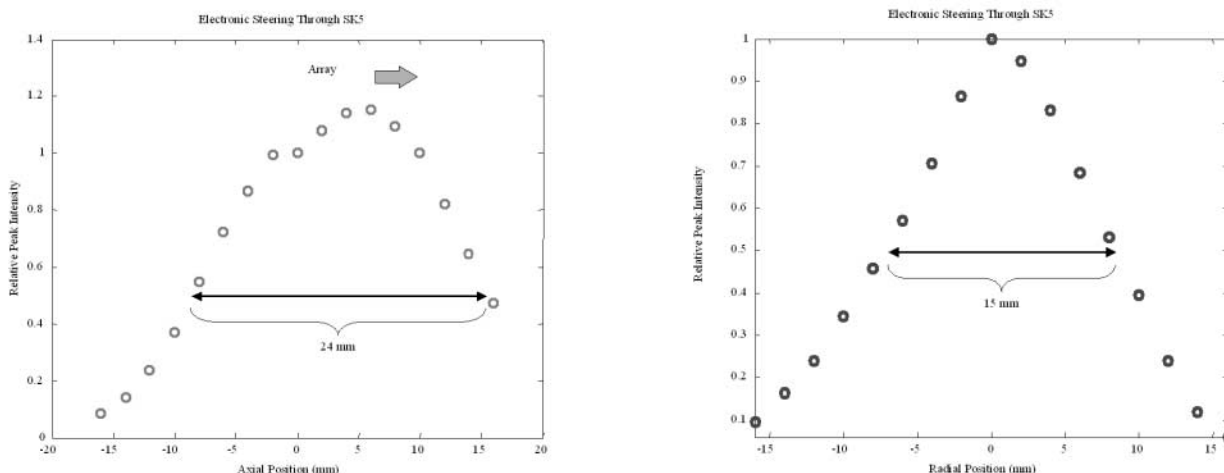
ed a steering range of 15 mm. This value is compared with the theoretical radial steering range of the transducer of 19 mm in water.

The thermocouple measurements on the skull and at the focus showed that a linear relationship existed between the duty cycle of sonication and the resulting temperature rise in the focus, whereas temperature rise in the skull remained negligible (<2°C for 100% duty cycle). Figure 5 shows the time history of the inner and outer skull surface temperatures during an 1800-W, 20-second sonication. This low overall temperature rise relative to the rise at the focus is evident in Figure 6A. It is also evident that a linear relation exists ($R^2 = 0.996$; $P < .01$) between the sonication power and the resulting temperature rise at the focus. Furthermore, the effect of increasing either parameter eventually leads to similar maximum temperatures (between 46°C and 51°C) by extrapolating the data for which sonication power is the independent variable to 1800 W ($R^2 = 0.999$; $P < .01$). Above 400 W, temperature readings were affected by cavitation artifacts caused by the thermocouple and were excluded. This extrapolation is represented in Figure 6B as a dashed line above 600 W. For increasing sonication times, the data showed no clear relationship between increasing power levels and the resulting temperature change but rather showed that the focus temperature rapidly ramps up and asymptotically approaches a steady-state temperature. This maximum temperature is dependent on several factors. In biological systems, the maximum temperature is determined by the dissipation of heat through blood circulation. The temperature change on both surfaces of the skull in every case is less than 6°C (this is 21% of the maximum temperature rise at the focus).

Two-dimensional temperature maps were next acquired with the use of MR thermometry to register temperature rises everywhere inside the phantom brain material. This procedure was executed with high-power sonications for 5 skulls in the MR imaging magnet. The resulting temperature elevations were highly localized, thus causing no excess heating away from the intended focal region. Figure 7 shows the temperature changes in a brain phantom due to a 20-second, 400-W sonication with phase correction. The average spatial and temporal profiles, respectively, are shown for the mean temperature rise in a 3×3 -voxel region of interest cen-

Figure 3. Pressure-squared intensity plots of 5 foci produced through a human skull by noninvasive focusing and beam steering. Target focal points are indicated with circles.





A **B**
Figure 4. Relative peak intensity as a function of distance from an initial point roughly centered within the skull in the axial (A) and radial (B) positions. Values are normalized to the intensity of this initial point.

tered around the focus. Error bars indicate the SD, and results indicate a peak temperature rise of approximately 20°C.

Discussion

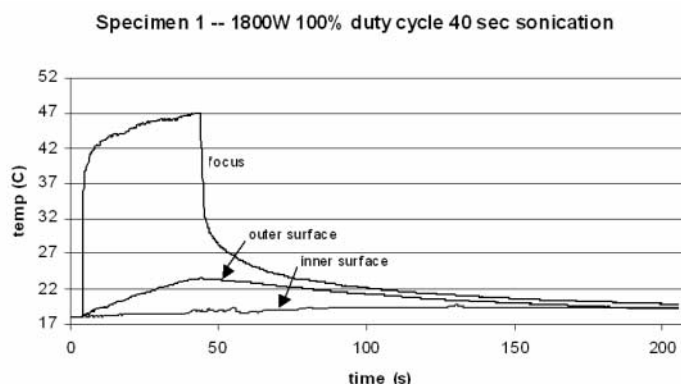
The 30-cm-diameter, 0.81-MHz hemispheric transducer divided into 500 elements was found to be sufficient for focusing through human skulls without producing excess heating of the skull surfaces and confirmed the results of previous virtual array experiments.⁹ In addition to this focal correction, the array was able to electronically steer the focus over a volume of approximately 30 × 30 × 26 mm. This volume was in general agreement with numeric field simulations of the transducer. Electronic shifting through the skull revealed an interesting combination of 2 uses for a phased array: aberration correction and beam steering.

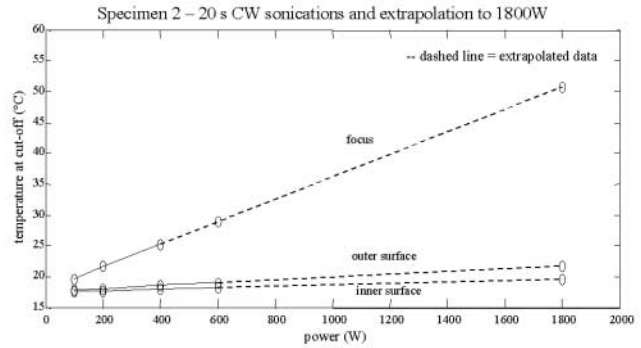
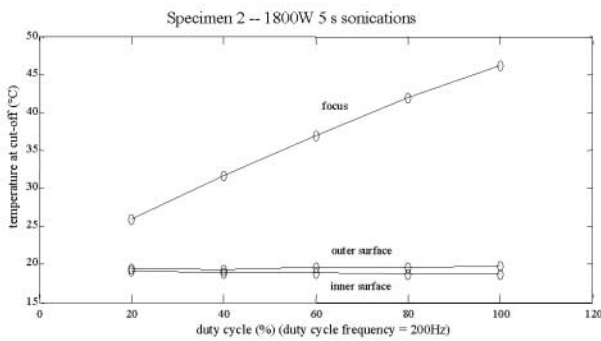
According to the results, the steering ranges through the skull are only slightly less than those expected in water without the skull present. The range suggests 2 things: the assumptions leading to Equation 1 are valid over the distances tested, and the element geometry and configuration of the array are the major limiting factors. It is possible that this steering ability could be greatly enhanced with a new array design optimized for range; however, the primary design consideration of the present array¹¹ was to achieve a focus through the skull.

High-power experiments with the array

showed how it may be used in conjunction with noninvasive focusing methods. The array was able to produce and steer a focus while operating at intensities high enough to coagulate and destroy brain tissue. At the same time, and most importantly, it did produce temperatures high enough on the skull surface to harm the surrounding tissue and the skin across the scalp.¹⁴ Considerable temperature increases were not observed on either the inner or outer skull surfaces when sonicating at high power. Results also indicate that this specific transducer array is compatible with MR-guided thermal imaging. The combined results provide evidence that the 500-element array can be used to focus through human skull bone under MR guidance.

Figure 5. Temperature as a function of time on the inner and outer skull surfaces and at the ultrasound focus.





A

B

Figure 6. Temperature at time of ultrasound cutoff on the inner and outer skull surfaces and at the ultrasound focus. The experiment was performed for 5 seconds at 1800 W with varying duty cycle percentages (A) and continuously for 20 seconds at powers up to 400 W (B) and then extrapolated to 1800 W (to avoid cavitation-induced heating artifacts produced with longer sonication times at high power).

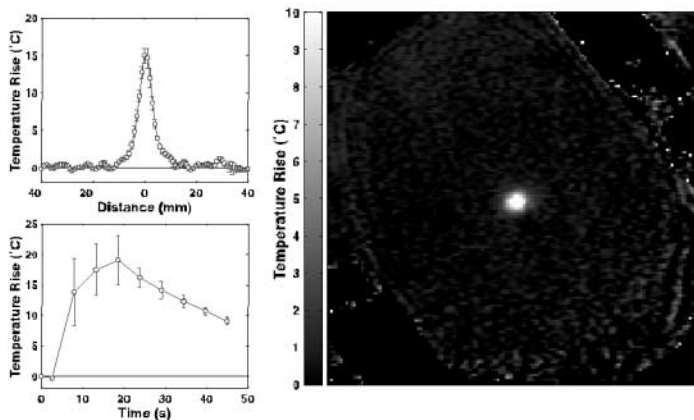


Figure 7. Temperature change through the skull due to a 20-second, 400-W sonication. Radial measurement (top left), axial measurement (bottom left), and MR thermal image (right) profiles represent the mean temperature rise in a 3 × 3-voxel region of interest centered around the focus. The error bars indicate SD.

- Clement GT, Hynynen K. A noninvasive method for focusing ultrasound through the human skull. *Phys Med Biol* 2002; 47:1219–1236.
- Aubry JF, Tanter M, Pernot M, Thomas J-L, Fink MA. Experimental demonstration of noninvasive transskull adaptive focusing based on prior computed tomography scans. *J Acoust Soc Am* 2003; 113:84–93.
- Thomas J-L, Fink MA. Ultrasonic beam focusing through tissue inhomogeneities with a time reversal mirror: application to transskull therapy. *IEEE Trans Ultrason Ferroelectr Freq Control* 1996; 43:1122–1129.
- Fry FJ. Transskull transmission of an intense focused ultrasonic beam. *Ultrasound Med Biol* 1977; 3:179–184.
- Sun J, Hynynen K. The potential of transskull ultrasound therapy and surgery using the maximum available skull surface area. *J Acoust Soc Am* 1999; 105:2519–2527.
- Sun J, Hynynen K. Focusing of therapeutic ultrasound through a human skull: a numerical study. *J Acoust Soc Am* 1998; 104:1705–1715.
- Clement GT, White JP, Hynynen K. Investigation of a large area phased array for focused ultrasound surgery through the skull. *Phys Med Biol* 2000; 45:1071–1083.
- Clement GT, Sun J, Giesecke T, Hynynen KH. A hemisphere array for non-invasive ultrasound brain therapy and surgery. *Phys Med Biol* 2000; 45:3707–3719.

References

- Fry FJ, Sanghvi NT, Morris RF, et al. Focused ultrasound system for tissue volume ablation in deep seated brain sites. In: *IEEE 1986 Ultrasonics Symposium Proceedings*. Piscataway, NJ: Institute of Electrical and Electronics Engineers; 1986.
- Hynynen K, Vykhodtseva NI, Chung AH, Sorrentino V, Colucci V, Jolesz FA. Thermal effects of focused ultrasound on the brain: determination with MR imaging. *Radiology* 1997; 204:247–253.

11. Clement GT, Hynynen KH. Criteria for the design and calibration of large area arrays for transskull ultrasound surgery and therapy. In: IEEE 2000 Ultrasonics Symposium Proceedings. Vol 2. Piscataway, NJ: Institute of Electrical and Electronics Engineers; 2000:1243–1246.
12. Clement GT, Hynynen K. Micro-receiver guided transcranial beam steering. IEEE Trans Ultrason Ferroelectr Freq Control 2002; 49:447–453.
13. Madsen EL, Frank GR, Dong F. Liquid or solid ultrasonically tissue-mimicking materials with very low scatter. Ultrasound Med Biol 1998; 24:535–542.
14. Moritz AR, Henriques FC Jr. Studies of thermal injury, II: the relative importance of time and surface temperature in the causation of cutaneous burns. Am J Pathol 1947; 23:695–720.